A rapid fluorescence based method for the quantitative analysis of cell culture media photo-degradation. A. Calvet, B. Li, and A.G. Ryder. *Analytica Chimica Acta*, 807, 111-119 (2014). **DOI**: 10.1016/j.aca.2013.11.028

A rapid fluorescence based method for the quantitative analysis of cell culture media photo-degradation.

Amandine Calvet, Boyan Li, and Alan G. Ryder. *

Nanoscale BioPhotonics Laboratory, School of Chemistry, National University of Ireland, Galway, Galway, Ireland.

* Corresponding author: **Email:** alan.ryder@nuigalway.ie **Phone:** +353-91-492943.

Postal address: Nanoscale BioPhotonics Laboratory, School of Chemistry, National University of Ireland, Galway, University Road, Galway, Ireland.

Running Title: Quantitative analysis of media photodegradation.

ABSTRACT:

Cell culture media are very complex chemical mixtures that are one of the most important aspects in biopharmaceutical manufacturing. The complex composition of many media leads to materials that are inherently unstable and of particular concern, is media photo-damage which can adversely affect cell culture performance. This can be significant particularly with small scale transparent bioreactors and media containers are used for process development or research. Chromatographic and/or mass spectrometry based analyses are often time-consuming and expensive for routine high-throughput media analysis particularly during scale up or development processes.

Fluorescence excitation-emission matrix (EEM) spectroscopy combined with multi-way chemometrics is a robust methodology applicable for the analysis of raw materials, media, and bioprocess broths. Here we demonstrate how EEM spectroscopy was used for the rapid, quantitative analysis of media degradation caused by ambient visible light exposure. The primary degradation pathways involve riboflavin (leading to the formation of lumichrome, LmC) which also causes photo-sensitised degradation of Tryptophan, which was validated using high pressure liquid chromatography (HPLC) measurements. The use of PARallel FACtor analysis (PARAFAC), multivariate curve resolution (MCR), and N-way Partial Least Squares (NPLS) enabled the rapid and easy monitoring of the compositional changes in tryptophan (Trp), tyrosine (Tyr), and riboflavin (Rf) concentration caused by ambient light exposure. Excellent agreement between HPLC and EEM methods was found for the change in Trp, Rf, and LmC concentrations.

Keywords: Cell culture media, Fluorescence, photo-degradation, riboflavin, chemometrics, PARAFAC.

1. Introduction

Chemically defined media (CD-media) are widely used in industrial mammalian cell culture and comprise an integral element of the manufacturing process. These CD-media are usually highly complex mixtures, containing amino acids, carbohydrates, vitamins, and other materials [1-4]. An enriched basal RDF (eRDF) media is one such example, which has relatively high concentrations of amino acids and glucose to sustain high density growth [5]. eRDF can vary in composition but typically comprises in excess of 30 different chemical species [6, 7]. It has been previously noted that these media are not chemically stable [8], but can undergo some slow rate chemical reactions when stored in the dark between 2-8°C, the industry standard temperature for storing large volumes of cell culture media. It is also well-known that cell culture media, and particularly those containing riboflavin are very sensitive to photo-chemically induced changes which can adversely affect cell growth [9-13]. Thus monitoring media stability is critical at a variety of stages in the development and manufacture of biological APIs. One generally develops and refines biologics manufacture on a small scale, paying particular attention to the generation of the best possible cell culture media that optimizes yield yet retains the other critical quality attributes required (*e.g.* glycosylation). Often this development work is undertaken with the use of transparent bioreactors, media storage vessels, or single-use disposable bioreactors [14], which can be transparent to wavelengths of light that can induce photo-damage.

Ideally for detailed analysis of media changes one would utilize chromatographic methods for the identification of specific component changes. For example a recently reported study on retinoic acid stability in cell culture media used a HPLC method which required a ~40 minute runtime per sample after a very complex and multi-step sample handling procedure [15]. Another time-consuming approach is to use metabolomics based methods to generate a high resolution picture of the composition [16]. These types of methods are often not practical from a cost/time consideration particularly the media quality for multiple small scale bioreactors has to be analyzed over days or weeks. What is needed is a rapid, inexpensive method capable of first detecting the onset of photo-damage and second quantifying the degree of change. We suggest using a combination of excitation-emission matrix (EEM) spectroscopy with multi-way chemometrics methods for rapid monitoring of media change [17]. The efficacy of EEM combined with chemometric methods for the identification, quality analysis, and quantification of various constituents of cell culture media has been established [8, 17-19]. EEM-chemometric methods are an ideal process analytical technology for the assessment of critical quality and performance attributes of the complex materials used to prepare cell culture media [20-24]. Raman spectroscopy can also be used for the identification and quality monitoring of CD-media [25, 26]. However, conventional Raman spectroscopy does not have sufficient sensitivity for measuring the small changes in the photophysically active analytes which are only present in low concentrations for many media. Here we demonstrate methods for using EEM methods to rapidly identify, monitor, and quantify both photo-chemically and chemically induced changes in cell culture media. Furthermore, EEM measurements can provide quantitative analysis [19] of some specific photo-active species present in media such as riboflavin (Rf), tryptophan (Trp), and tyrosine (Tyr). The ability to rapidly identify and quantify variances in the concentrations of

these fluorophores in the complex cell culture media is of interest from both quality control and quality assurance points of view. These rapid spectroscopic methods provide a relatively inexpensive and rapid approach for media monitoring over extended timeframes, which should be of particular use during process development, scale up and general operations in biotechnology.

2. Materials and Methods

2.1 Materials: eRDF was obtained from Kyokuto Pharmaceuticals Industrial (Japan). NaOH (97+ %), $NaHCO_3$ (99.7+ %), L-tyrosine (≥ 98%), L-tryptophan (≥ 98%), pyridoxine, (-)-riboflavin and folic acid dihydrate (97 %) were obtained from Sigma-Aldrich and used without further purification. An aliquot of sterilized high purity water was used to dissolve eRDF (4.4248 g), to which was added $NaHCO_3$ (0.2832 g) before making the solution up to a final volume of 250 mL (17.7 g/L working concentration, eRDF stock). The solution was immediately sterilized by membrane (0.22 μm) filtration and then dispensed as 1.25 mL aliquots into sterile containers (2 mL translucent polypropylene eppendorf tubes) before being placed in one of the four storage conditions: *1).* RT-L: Room temperature in the light; *2).* RT-D: Room temperature in the dark; *3).* C-L: Cold (Fridge) with light, and *4).* C-D: Cold (Fridge) in the dark. Control samples were stored in the dark at -70ºC.

The dark stored samples were placed in a cardboard box covered with tin foil at all times. For the light exposed samples, a similar light source was used inside and outside of the fridge: Phillips warm white 827 Genie stick energy saving bulb (420 lumen) on for 24 hours a day (Figure S1, *supplemental information*). The temperatures inside and outside the fridge were recorded throughout the experiment and the room temperature (r.t.) samples were kept at 16.4±3.0ºC whereas the fridge temperature 6.0 ± 1.5ºC. The temperature variation in the fridge is explained by the necessity to have the power inlet for the lamp hindering perfect closure. The four boxes containing the samples were rotated regularly in order to prevent inequalities between sample *vis-à-vis* temperature and light exposure conditions. Fluorescence EEM spectral data were collected over 32 days (Day 0, 7, 11, 14, 18, 21, 25, 28, and 32). At every sampling point three samples were removed from each of the four storage conditions and immediately placed in the dark at 4ºC to limit any further change in the samples during the 3-4 hour time period required to collect the EEM from the 12 samples in random order.

2.2 Sample preparation for calibration: For the quantification of Tyr, Trp, Rf, folic acid (FA), and pyridoxine (Py) in the photo-degraded eRDF we used a NPLS quantitative method in which the calibration samples were generated from spiked eRDF solutions.[19] The method was extended in this study to quantify of Py, Rf, and FA. In this method a *Test* (reference) 17.7 g/L eRDF solution was spiked 10 times in order to triple the initial analyte concentration (c_0). This lead to a total of 31 samples comprising a *Test* sample and 10 spiked samples for each analyte. The EEM of these samples were collected in triplicate and then used for calibration (dataset **quant_cal**). A second, independently prepared dataset (**quant_pred**) was used for prediction (see *supplemental information* for details).

2.3 Fluorescence instrumentation and data collection: EEM were measured over various excitation and emission spectral ranges with a data interval of 5 nm using a Cary Eclipse

(Varian) fluorescence spectrometer with semi-micro quartz cuvettes[1] [8]. The EEM matrices varied according to the specific target analytes being analyzed *e.g.* for amino acids, dataset **AFaa**): λ_{ex} = 220–400 nm/λ_{em} = 250–600 nm/slit widths = 5 nm; for the vitamins, dataset **AFv**: λ_{ex} = 315–540 nm/λ_{em} = 330–600 nm/slit widths = 5 nm (ex.) / 10 nm (em.).

2.4 Chemometric methods and data analysis: All calculations were performed using PLS_Toolbox 4.0®, supplemented by in-house-written MATLAB® (ver. 7.4) code. The NPLS quantification methods used modified standard addition method (*MSAM*),[27, 28] and unfolded principal component analysis (UPCA) which have been described in detail elsewhere [19]. Calibration model performance was assessed using both root mean square errors of validation (RMSEV), and prediction (RMSEP).

2.5 High Performance Liquid Chromatography (HPLC): The HPLC system was an Alliance chromatographic separation unit (waters 2689) equipped with a UV detector (2487). The column used was a 4.6x150 mm Sunfire C18 column with 5 µm particle size. For the 10 first minutes a 85:15 mixture of 0.05 M KH2PO4 in milli-Q® water and methanol was used, followed by a 7:3 mixture of water and methanol for another 50 min. Each run was 70 minutes long which included a 10 minute equilibration between injections. A 1.0 mL/min flow was kept constant throughout the run, and three injections per sample were made. Two UV detection channels were used: 275 nm for the detection of tryptophan (Trp) and 360 nm for the detection of riboflavin (Rf) and lumichrome (LmC). Calibration curves were prepared for each of Trp, Rf, and LmC over the relevant concentration ranges. The Trp calibration curve had an R^2 of 1.00, with an Relative Standard Deviation (RSD) of 0.47% (fit equation, $y=1.71\times10^4x+9.20\times10^3$). The Rf calibration curve had an R^2 of 0.99, with an RSD = 1.7% (fit equation, $y=2.60\times10^4x-9.65\times10^3$). For LmC the values were R^2 = 0.922, RSD = 14.1% (fit equation, $y=1.74\times10^4x-9.65\times10^3$).

3. Results and Discussion

3.1 Spectral changes caused by photo-degradation: eRDF EEM solution spectra are very complex with the strongest emission from Tyr and Trp, and weaker contributions at longer excitation and emission wavelengths from Py, Rf, and FA [19]. When eRDF solutions were exposed to ambient room light very significant changes occured quite rapidly, and we observed (Figure 1) the formation of a new broad fluorescence band with excitation/emission at 360/460 nm (there are two weaker excitation bands at 240 and 260 nm associated with this emission). The EEM difference spectra (Day32–Day0) show this more clearly, as well as a significant decrease in Trp emission (there is also a small noticeable decrease in Tyr emission). The rate of increase of this new band is significantly fast when the media is exposed to light and can be easily identified using chemometric methods (*vide infra*).

[1] In this set up a 4 mm excitation pathlength and 10 mm emission pathlength were used.

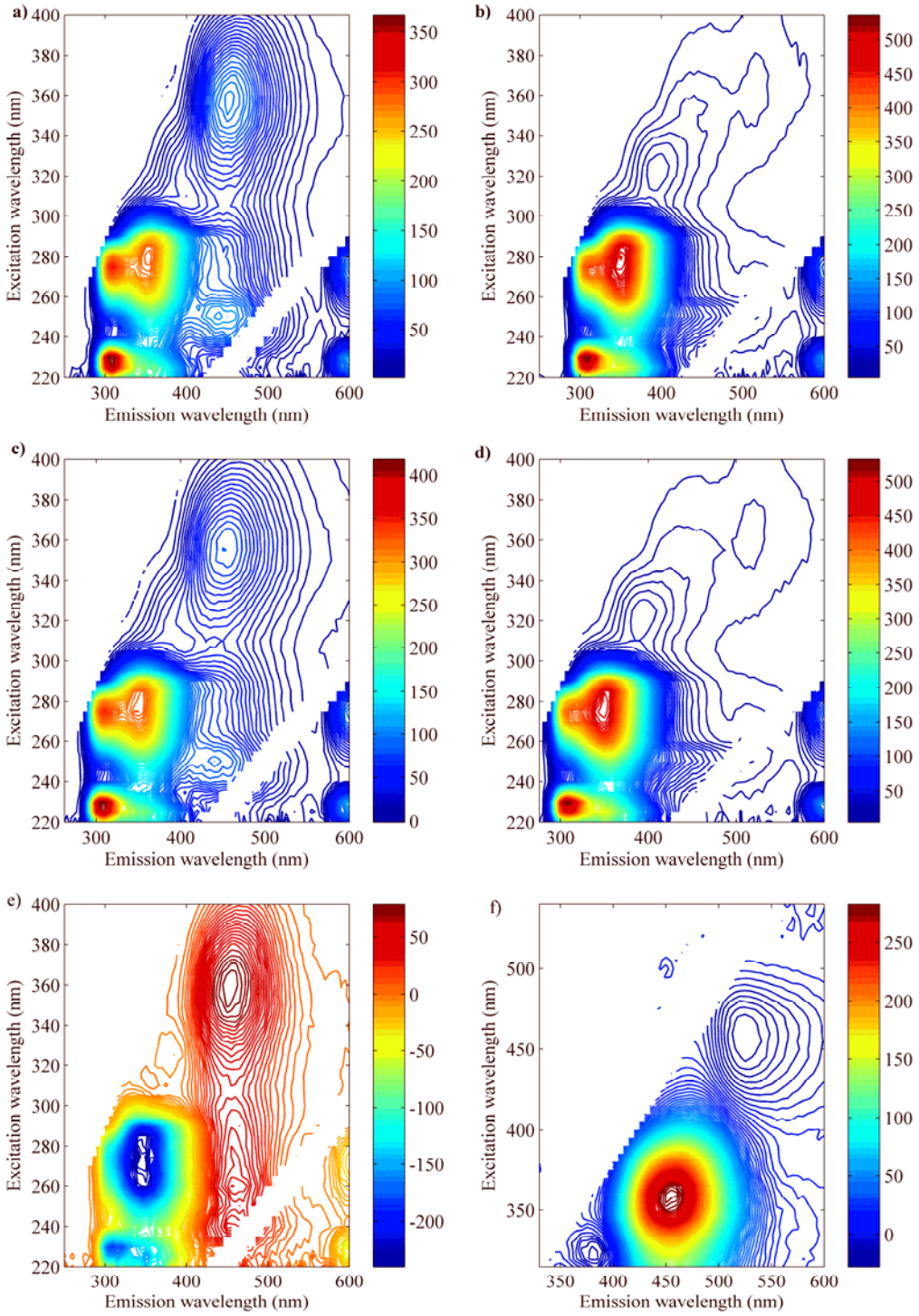

Figure 1: EEM landscape plots from selected eRDF solutions (17.7 g/L) in the amino acid region (***AFaa***). ***Top row***: samples stored at room temperature for 32 days in the light (a) and dark (b). ***Middle row:*** samples stored in the fridge for 32 days in the light (c) and dark (d). ***Bottom Row***: Difference EEM contour plots (Day32–Day0) of light exposed/room-temperature eRDF solution for the two different spectral regions measured (***AFaa, AFv***).

The possible photo-products arising from the photo-degradation of Trp, Tyr, and Rf described in the literature are listed in the supplemental information (Table S3, *supplemental information*). Lumichrome (LmC) is the compound that best explains the fluorescence band

appearing at 360 nm (ex.) / 450 nm (em.) in the irradiated solution EEM, and this agrees with literature observations, and HPLC measurements (*vide infra*) [16, 29-31]. The large decrease in Trp signal is indicative of significant degradation, probably caused by the formation of reactive oxygen species by photo-excited riboflavin [10, 32]. The most likely photo-products are N-formyl kynurenine (NFK) and5-hydroxytryptophan (5-HTP) with the possibility of tetrahydropentoxyline also being formed [16, 33, 34]. Hydroxy-kynurenine (HOK) was also found to be a Trp photo-product in the degradation of wool [35]. The tyrosine signal is also reduced, and a potential, direct photo-product is dityrosine [36, 37].

3.2 Modelling of eRDF degradation: To better characterize the spectral composition changes we used PARAFAC modelling of the EEM data collected from all the eRDF solutions [38, 39]. First a PARAFAC, 4-factor model, was used to look at the widest EEM range and is thus dominated by Trp/Tyr emission (Figure 2). It is clear that factors 1 and 2 correspond to Trp and Tyr emission respectively while factor 3 looks like a distorted Py emission band (compared to the PARAFAC model of fresh eRDF solutions, [19]). The fourth factor covers the emission range where we might expect to observe the weak FA and Rf emission in the fresh media [19]; however, its appearance and behaviour suggest that this is in fact, emission arising from some of the photo-products. This is borne out by the scores plots which show that this component is very weak for the dark-stored samples, but when exposed to light, this component becomes the dominant factor. Thus irrespective of the specific source of the factor 4 signal, we can use the change in the scores of this factor as a direct measure of media photo-degradation. It is important to note that, these changes in fluorescence response as measured by PARAFAC scores cannot always be simply related to specific changes in the fluorophore concentration. Changes in concentration of other chromophores and fluorophores will affect the fluorescence emission of species without affecting their concentration, for example by inducing extra absorption related Inner Filter Effects (IFE).

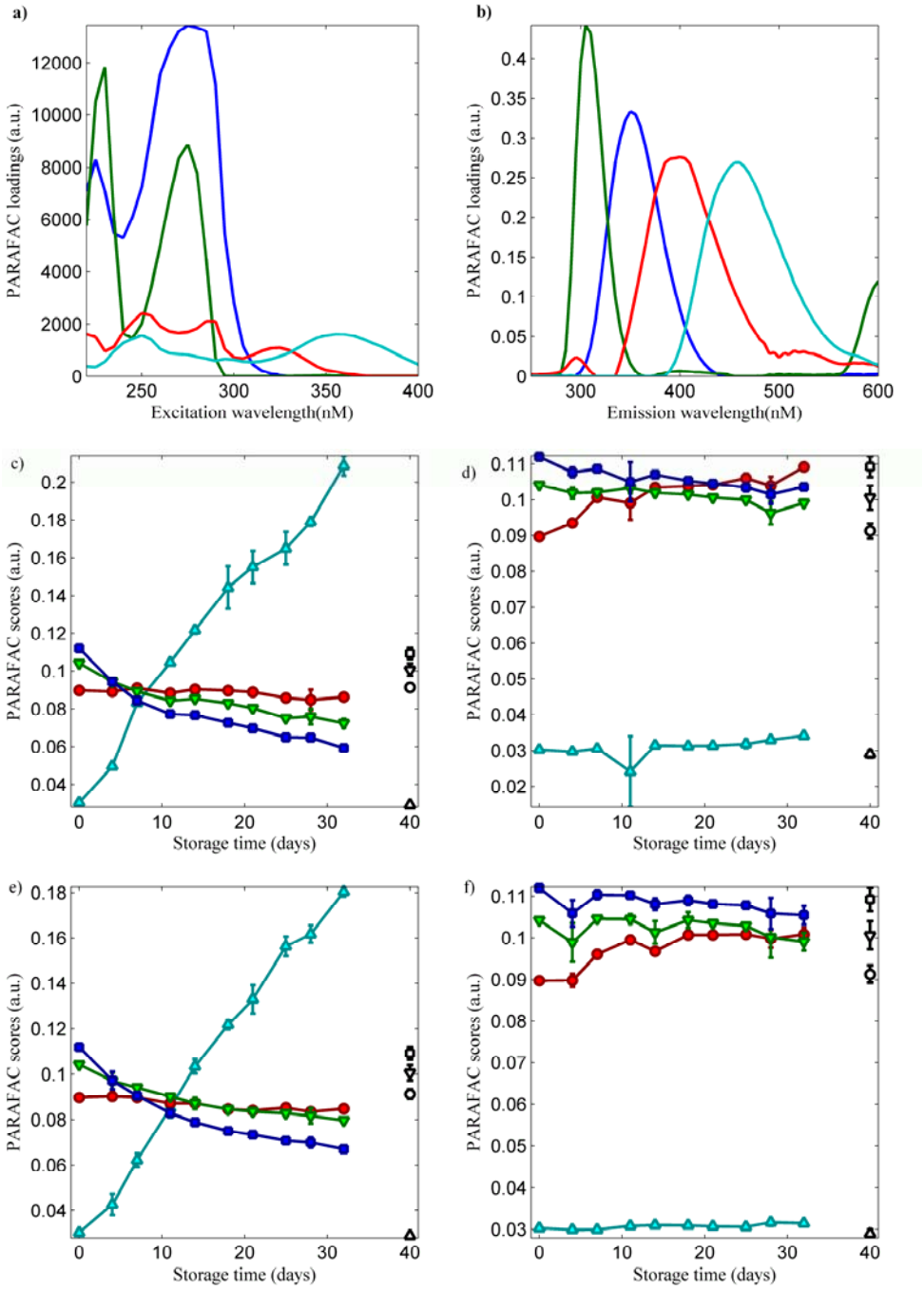

Figure 2: Excitation (a) and emission (b) loading of the **AFaa** PARAFAC model with 4 components. Components 1 to 4 are represented by blue squares (Trp), green inverted triangles (Tyr), red circles (Py), and cyan upright triangles (FA/Rf and/or photo-products) respectively. The PARAFAC scores are shown for the four different storage conditions: *(a)* RT-L, *(b)* RT-D, *(c)* C-L, and *(d)* C-D. The control samples (stored in the dark at-70ºC) are arbitrarily shown at day 40 for comparison on each plot. The model used non-negativity constrains on all modes, explained 99.9 % of the total spectral variance, and had a core consistency of 19.

The scores plots show as expected (from the Rf photosensitised degradation pathway) that there are very large changes in Trp emission due to photo-degradation and over 32 days we see a 47 % drop in Trp relative intensity at r.t. in the light, but only a 6% decrease in the cold dark storage condition (Figure 2c-d). The difference between the cold and r.t. stored

samples is very small, but after 32 days (dark) both are significantly less than the -70°C stored controlled samples. This is probably due to photo-degradation occurring during sample preparation (~4 hours) and handling, and is supported by the slight increase of the photo-product signal (factor 4, Figure 2) concurrent with the signal decrease of the intrinsic fluorophores (Trp and Tyr). However other chemical degradation pathways are also expected as these complex chemical mixtures in the liquid state will undergo collisional induced reactions [8]. Tyr displays a similar behaviour, with a 31 % drop of relative intensity for warm-light storage and only a 5 % drop in the cold-dark.

It is important to note that in a complex medium, such as eRDF, the precise relationship between changes in fluorescence emission and analyte concentration changes is not always easy to decipher. The chemical changes induced by light absorption results in concentration changes in both intrinsic fluorophores and fluorescent photo-products, both of which are clearly seen in the EEM plots. However, secondary effects caused by changes in absorption (*e.g.* IFE) and changing quenching rates are also present and these have to be considered. When we compare the absorption spectra of the fresh and 21 day light aged eRDF solutions (Figure S-3, *supplemental info*) we see significant increases in light absorption between 240 and 320 nm, and very little change above 400 nm. Based on the increase in absorption only, we can estimate that IFE would be responsible for decreases of 25 and 22 % in emission signal for Trp and Tyr respectively over 21 days. However, the PARAFAC model shows 38 and 23 % decreases respectively, for Trp and Tyr, which is again clear evidence for Trp is photo-degradation.

For Tyr it is interesting to note that only ~1 % of PARAFAC Tyr signal drop is ascribed due to photo-degradation when absorption IFE is considered. It is known that Tyr can also be photo-degraded by Rf and oxygen in a similar fashion, but at a slower rate than Trp [40]. However dityrosine formation (300 nm excitation and 400 nm emission [37] was not observed and this is consistent with the results from a previous study of cell culture media degradation [16]. The third component which is similar to Py emission behaves very differently in that there is virtually no change when exposed to light at r.t. or in the cold, but we observe some significant increases in apparent emission when stored in the dark. However changes in the Py emission is better modelled using a narrower spectral region (AFv), (Figure 3). The fourth factor in the PARAFAC model (AFaa dataset) is obviously associated with the generation of several photo-degradation product(s). From the appearance of the loadings plots it is obvious that there are at least two emitting species in this fourth component. PARAFAC on the wide EEM spectral range cannot clearly resolve these species probably because the Trp and Tyr, responsible for over 70 %[2] of the signal in this EEM region, obscures the longer wavelength photo-products emission. To better resolve the signal corresponding to this component we reran PARAFAC on the smaller EEM range (AFv) which excludes much of the Trp/Tyr signal. However, neither 4 factor (*supplemental information*) nor 5 factor models were good. The 5 factor model was not stable (and core consistency <0) probably due to the collinearity between the excitation component of several fluorophores making PARAFAC unfit for the modelling of this dataset.

[2] Calculated based on the % of X explained by the 2 first component in the PARAFAC model.

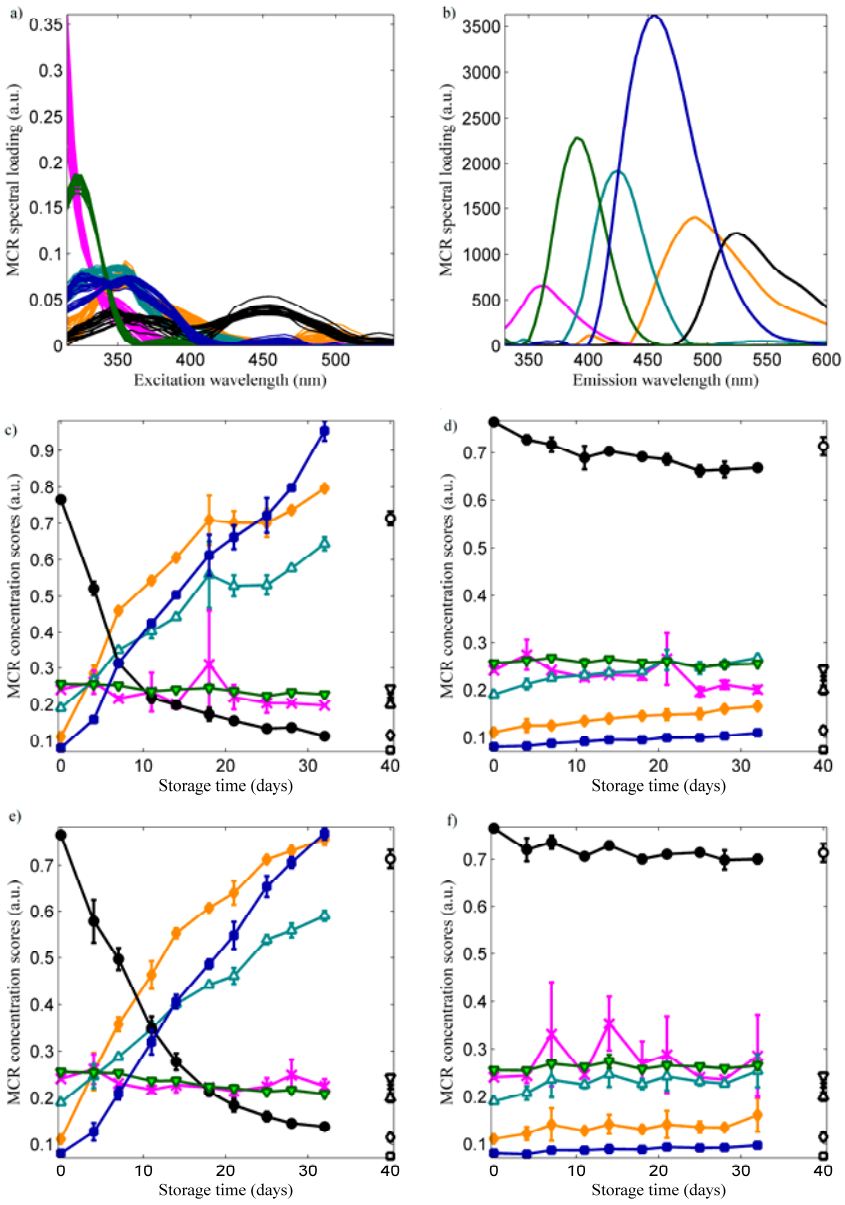

Figure 3 6-factor MCR-ALS model of the **AFv** dataset. ***Top row:*** (a) excitation and (b) emission loadings. ***Middle row:*** Scores plots for samples at room temperature exposed to light (c) and in the dark (d). ***Bottom row:*** Scores plots for samples at low temperature exposed to light (e) and in the dark (f). Factors 1 to 6 are represented in blue (■), green (▼), red (◯) and cyan (▲),magenta (x) and orange (♦) respectively. The controls (-70ºC) are arbitrarily shown at day 40. The model used non-negativity constrains on both modes.

To solve this issue we implemented Multivariate-Curve Resolution (MCR) on the augmented AFv matrix with the emission variables as the 'spectral' mode and the combined excitation and sample variables as the 'concentration' mode. AFv was found to be best fitted with a 6 factor model (Figure 3). In Figure 3, the formation of LmC (factor 6) as a response to the riboflavin degradation (factor 3) is evident and the formation of two other degradation products is also visible (factor 4 and factor 1). It is clear that restricting the EEM range to the longer wavelength range gives a much clearer view of the evolution of the degradation

products. We observed three distinct fluorescent degradation products, and the excitation and emission loadings obtained for the MCR model were ascribed to the following species: Hydroxy-kynurenine (HOK),[41] N-Formyl-kynurenine (NFK), Py, LmC,[16] and Rf (Table 1, and *supplemental information*). However loss in the Trp signal is not clear in Figure 3 and this is due to the fact that the Trp signal in this dataset only includes the Trp excitation tail above 315 nm. Furthermore, the low quantum yields and extinction coefficients of the Trp photo-products are offset by the fact that Trp concentration is 150 times that of Rf. Thus the kynurenine derivatives should have an equivalent impact to that of LmC on the EEM spectra. The NFK and LmC factor scores are not zero for the starting point nor for the control samples because of photo-damage occurring during sample preparation.

The observed decrease of the Rf signal (factor 5) during storage is very significant with light, (for RT-L it is ~85 % after 32 days) compared to when the medium is kept in the dark (13 % in C-D after 32 days,). The rate of decrease is also greater at r.t., with the Rf emission reduced by 50% in less than 7 days whereas at 6 ºC, it took ~10 days for a 50 % reduction in signal. Concurrent with Rf removal, we see an increase in signal for LmC (factor 6) that is inversely related to the change in the Rf MCR scores. This is direct evidence for LmC formation from Rf photo-degradation. The scores of the other two factors (4,1) does not follow this trend indicating a separate source for these products (kynurenine derivatives) *i.e.* they arise from Rf photo-sensitised degradation of Trp. LC/MS evidence for these pathways has been published [16]. The Py associated factor (#2) seems to be relatively constant irrespective of the storage conditions. The slight decrease in its scores for the light exposed samples is attributable to IFE caused by the generation of LmC and kynurenine photo-products Trp which all have significant molar absorptivity's in this spectral range. As above we also have to consider the IFE changes, and at the excitation wavelength maximum for Rf (365 nm) absorbance is increased by ~30 % over 21 days. This would lead to a 9 % reduction in the available excitation light and thus an equivalent decrease in emission intensity. This is not however, sufficient to explain the 77 % signal loss recorded, and thus we can safely conclude that Rf is being removed by photo-degradation.

To validate the fluorescence EEM observations that Rf/Trp degradation coupled with the production of lumichrome were the dominant processes, a quantitative HPLC study was undertaken. The Rf, Trp, and LmC levels in various samples stored at room temperature and under light exposure were measured. The linear range for Trp, RF, and LmC were 8.32 to 166.4 µM, 0.054 to 1.08 µM and 0.22 to 1.08 µM respectively. First non-photo-degraded samples were tested, and the concentrations of Trp and Rf measured in a control sample and a sample kept in the fridge in dark for 32 days were very similar (79.9/79.4 µM and 0.54/0.53 µM – control/FD) which is in agreement with the observed fluorescence data. After 32 days in the fridge in the dark the concentration of LmC was too low to be detected using this HPLC method. When the room temperature, light stored samples were tested we observed a linear decrease in Trp concentration (figure 4a), an exponential like decrease in Rf (figure 4b), and an increase in the concentration of lumichrome (figure 4b). When we then compared the HPLC concentration data with the recovered MCR scores (figure 4c-e) we observe a linear relationship for both the Trp and LmC. The case with Rf it is less certain

because as after 11 days the Rf concentration has decreased below the limit of detection for the specific HPLC method employed (Table 2).

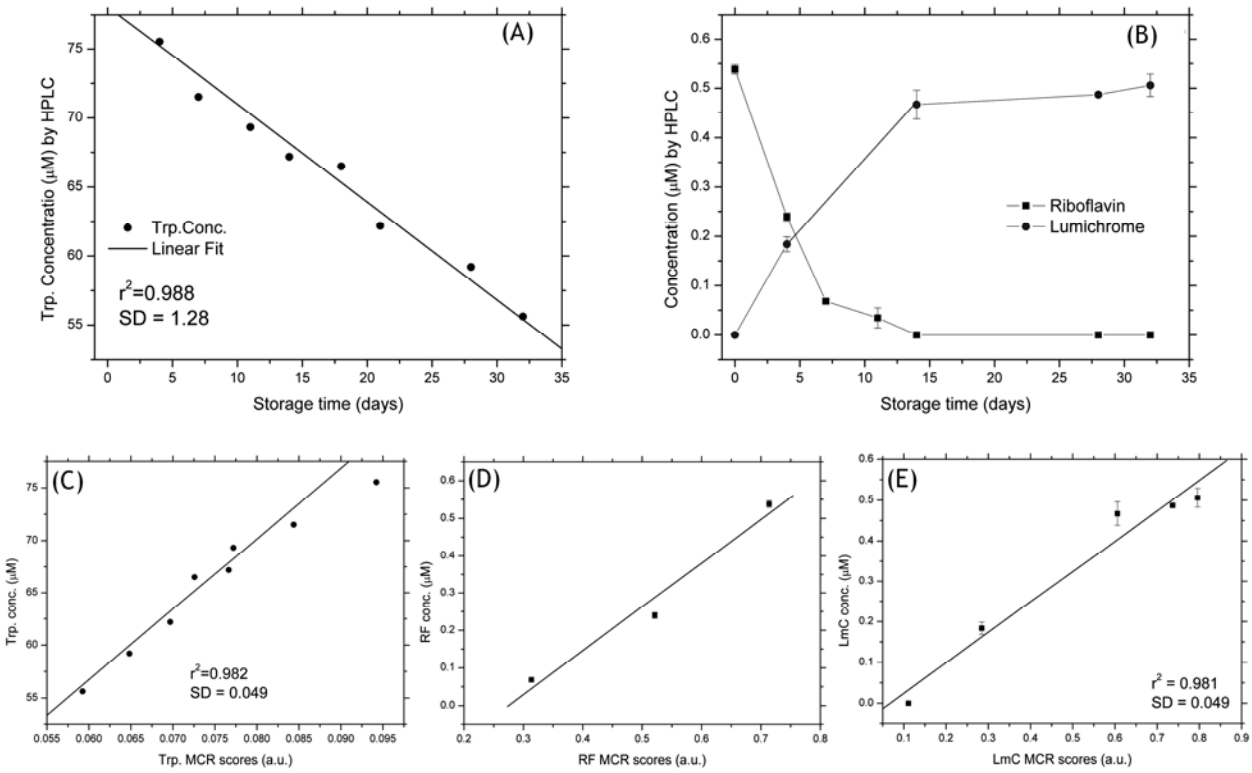

Figure 4: **(A)** Tryptophan, and (B) Riboflavin/Lumichrome concentrations measured by HPLC for media samples stored in the light at room temperature. The average of 3 injections per sample are shown (error bars are plotted). The data used for Lumichrome are those with relative standard deviations of less than 10% (n=3). After 11 days the Rf was not detectable using this HPLC method (the limit of detection was ~0.05 µM). (C-D) scatter plots showing the correlation between the measured concentrations of Trp, Rf, and LmC by HPLC with the recovered MCR scores for these components.

3.3 Quantification of components using EEM data : Trp and Tyr in eRDF solution can also be quantified by EEM using a previously demonstrated modified standard addition method [19]. NPLS [42] was used because it can handle some of the deviations from data tri-linearity caused by IFE and Radiative Energy Transfer [43]. Here we expanded the method to the quantification of Py, FA, and Rf in eRDF. For each of these analytes a large series of studies were undertaken in which we varied the spectral region sampled, the pre-processing steps, and NPLS model parameters. After this sequence of trial and error we determined the best quantitative models (**Table 3** & *supplemental information*) by considering the RMSEV and RMSEP values.

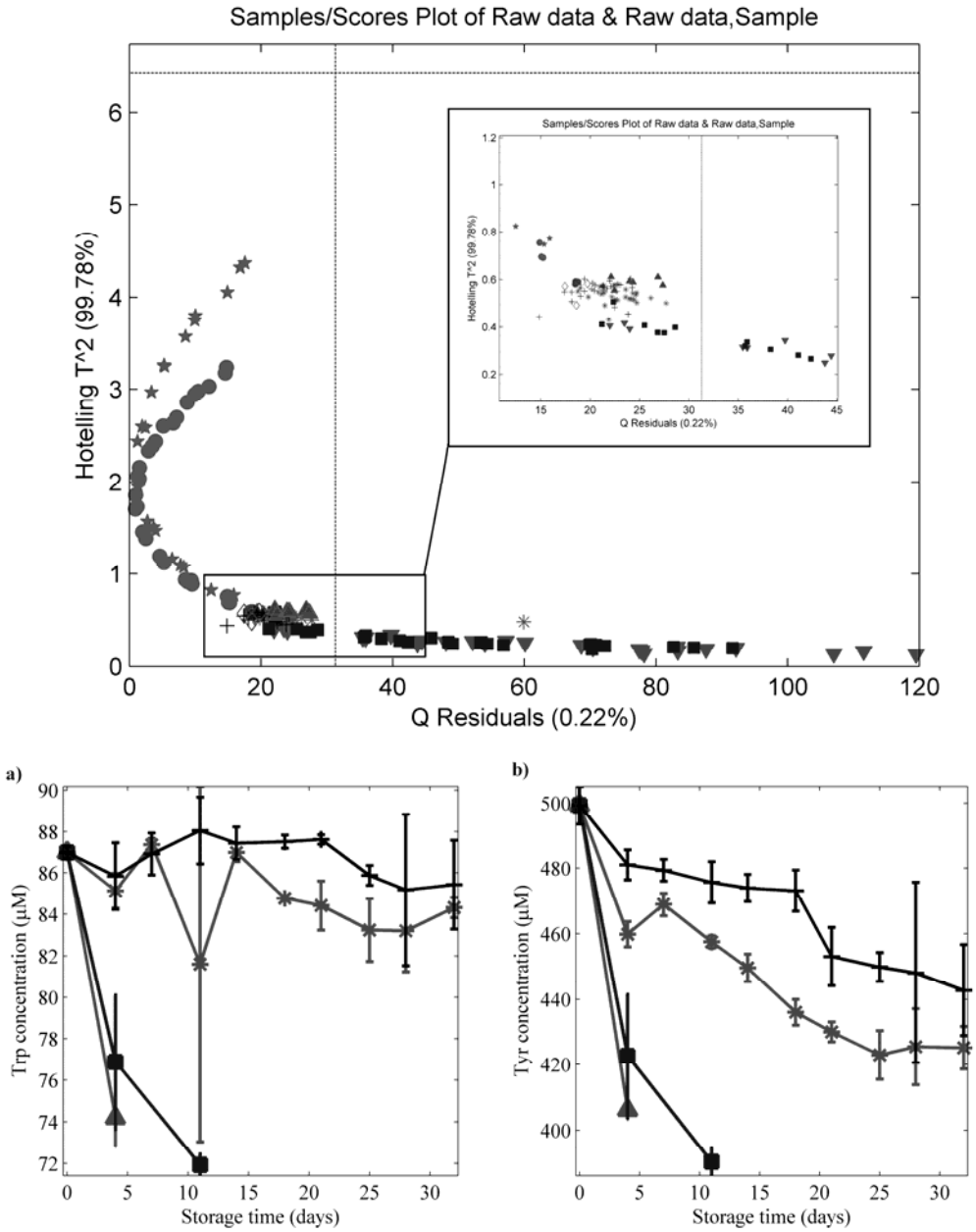

Figure 5: (Top) UPCA analysis (2 components) used for Tyr prediction of the photo-degraded 17.7 g/L eRDF. The calibration samples [non-spiked (▲), Trp spiked (●) and Tyr spiked (★)] and photo-degraded samples (RT-L (▼), RT-D (*), C-L (■), and C-D (+)) are shown. The model used a spectral range of 220-295 nm excitation and 305-495 nm emission region which was centred across the sample mode and scaled within the excitation mode**. (Bottom)** Predicted Trp (a) and Tyr (b) concentrations of non-outlying samples that were stored for several days in conditions) RT-L (▲), RT-D (*), C-L (■), and C-D (+).

Py and Rf could be determined with REP's of 4.6 and 2.3 % respectively, however the Py model uses as many as 8 LVs. In such complex samples, high numbers of latent variables is expected but it also raises the issue of over fitting. For this reason the FA and Py model were not used. Calibration for the determination of FA only led to REP of 8.7 % at best, and up to 12 LVs are required. This is due to the weakness of FA fluorescence and its strong

extinction coefficient source of high deviation to tri-linearity condition impacting all fluorophores. The Trp, Tyr and Rf models were then used for the quantitative analysis of the stored eRDF media solutions. One drawback in using these NPLS models for the analysis of the photo-degraded media is that only minimal variations from the matrix of the reference samples used in the calibration step are allowed. Therefore, we first had to assess the suitability of the aged eRDF media samples for use with these quantitative models. The EEM data collected from the stored media were analysed using UPCA models generated from the original calibration samples for each analyte determination (Trp, Tyr [19], and Rf). We used the resultant Hotelling T^2 *vs*. Q-residuals plots (T^2-Q plot, using a 95 % confidence limit) to select the samples which were suitable for quantitative analysis. Figure 5 shows the UPCA T^2-Q plot for the Tyr prediction model (*see supplemental information for details of the other analytes*). From this plot, it is obvious that the emission from samples stored in the light undergo much more change than the dark stored samples. For Tyr all the dark stored samples appeared to be fit for quantification using the MSAM-NPLS quantitative models (apart for a single outlier measurement). For the light exposed samples, the only samples found suitable for Tyr quantitative analysis were those exposed to light for less than 11 days at low temperature or four days at r.t. In practice, a more frequent sampling plan in the initial stages would be better for tracking the changes in analyte concentration for the light exposed samples. The predicted concentrations for the degraded and control samples are given in the supplemental information and shown graphically in Figure 5.

The rapid drop in concentrations of Trp under irradiation (~18 % after 7 days for Tyr and Trp respectively at r.t.) agrees with the PARAFAC results, with Trp undergoing photo-degradation leading to the formation of hydroxykynurenine, N-formyl-kynurenine [16], and probably other non-fluorescent compounds. When compared to the HPLC measurements, the NPLS method overestimates the concentration drop (-18% versus -10%), which is due to two factors. First the NPLS model was built using the formulation value as the Day 0 concentration, and second the large change in the matrix is obviously having an impact on accuracy as is the case for Tyr. For Tyr, the significant concentration drop plotted (Figure 5b) results from the fast changing fluorescence matrix and in particular the change in IFE (see above) rather than a real change in concentration. The Rf NPLS model was the only other model which was acceptable; however, when the stored samples were tested against the UPCA model (*supplemental information*) we found that none of the stored (dark or light) samples could be used for prediction as the degree of spectral/matrix change was too great. This indicates that this particular model is too sensitive to Rf concentration changes which is unsurprising since we used a very narrow spectral range centred on the Rf emission band for this model. These results also raise the possibility that photo-degradation of Rf is taking place very rapidly during the sample preparation and handling.

4. Conclusions

This study shows that fluorescence EEM coupled with multi-way chemometrics methods is a rapid, effective and inexpensive method for the quantitative analysis of cell culture media photo-degradation. The method requires minimum sample handling and only takes ~5 minutes per measurement which is considerably faster than high resolution HPLC or

mass spectrometry based approaches. PARAFAC/MCR-ALS provided an unambiguous measurement of the degradation process both by monitoring the decrease of intrinsic media components and the formation of photo-degradation products. Furthermore, the fluorescence data for Trp and Rf were in excellent agreement with the HPLC measurements. We do accept that these methods do not provide for unambiguous identification of many specific photo-products, however, the important issue is the identification and quantification of the degree of photo-damage. A detailed investigation into the specific materials degraded and the photo-products formed can then be undertaken using more expensive separations and mass spectrometry based approaches. In addition, it was possible to quantify the change in concentration in samples that were not extensively photo-degraded with a reasonable degree of accuracy using NPLS. However, for more degraded media, the method is not as accurate as the MCR based approach where there are good linear correlations between true concentrations and MCR/PARAFAC scores.

The combined benefits of being able to first determine photo-degradation and second being able to quantify low levels of degradation using EEM offers considerable benefits for routine quality assurance requirements during media formulation and operational use. In particular these methods will be of benefit for small scale bioreactor studies or where transparent single-use disposable bioreactors are often used. The low-cost, and short time required per analysis should facilitate implementation of simple control strategies to make small scale cell culture more reliable. This information can thus be used to trigger a more time-consuming and expensive chromatographic based investigation. These methods when coupled to previous research on qualitative analysis of media components [18], and correlating media variance with process performance [8] allows for the use of fluorescence EEM as a comprehensive analytical tool for biotechnology manufacturing.

5. Acknowledgements

AC acknowledges funding support from IRC (Irish Research Council). The HPLC system used in this work was donated by Boston Scientific (Galway) and refurbished with funding from Science Foundation Ireland.

6. Supplemental information available

Supporting information is available which included further details on the spectral and quantitative analyses.

7. References

[1] T. Cartwright, G. Shah, in: J.M. Davis (Ed.), Basic Cell Culture, Oxford University Press Inc., New York 2002, p. 69.
[2] K. Wlaschin, W. Hu, Cell Culture Engineering, 101 (2006) 43.
[3] E. Jain, A. Kumar, Biotechnol. Adv., 26 (2008) 46.
[4] G. Sitton, F. Srienc, J. Biotechnol., 135 (2008) 174.
[5] D. Jayme, T. Watanabe, T. Shimada, Cytotechnology, 23 (1997) 95.
[6] F. Chua, S.K.W. Oh, M. Yap, W.K. Teo, J. Immunol. Methods, 167 (1994) 109.
[7] P. Ducommun, P. Ruffieux, U. Von Stockar, I. Marison, Cytotechnology, 37 (2001) 65.

[8] P.W. Ryan, B. Li, M. Shanahan, K.J. Leister, A.G. Ryder, Anal. Chem., 82 (2010) 1311.
[9] R.J. Wang, J.D. Stoien, F. Landa, Nature, 247 (1974) 43.
[10] J.D. Stoien, R.J. Wang, Proc. Natl. Acad. Sci. U. S. A., 71 (1974) 3961.
[11] R.J. Wang, Photochem. Photobiol., 21 (1975) 373.
[12] B.T. Nixon, R.J. Wang, Photochem. Photobiol., 26 (1977) 589.
[13] A.M. Edwards, E. Silva, B. Jofre, M.I. Becker, A.E. Deioannes, J. Photochem. Photobiol. B-Biol., 24 (1994) 179.
[14] V. Singh, Cytotechnology, 30 (1999) 149.
[15] K.A. Sharow, B. Temkin, M.A. Asson-Batres, Int. J. Dev. Biol., 56 (2012) 273.
[16] L. Zang, R. Frenkel, J. Simeone, M. Lanan, M. Byers, Y. Lyubarskaya, Anal. Chem., 83 (2011) 5422.
[17] B. Li, N.M.S. Sirimuthu, B.H. Ray, A.G. Ryder, J. Raman Spectrosc., 43 (2012) 1074.
[18] B. Li, P.W. Ryan, M. Shanahan, K.J. Leister, A.G. Ryder, Appl. Spectrosc., 65 (2011) 1240.
[19] C. Calvet, B. Li, A.G. Ryder, J. Pharm. Biomed. Anal., 71 (2012) 89.
[20] J.A. Lopes, P.F. Costa, T.P. Alves, J.C. Menezes, Chemometr. Intell. Lab. Syst., 74 (2004) 269.
[21] A.P. Teixeira, R. Oliveira, P.M. Alves, M.J. Carrondo, Biotechnol. Adv., 27 (2009) 726.
[22] E. Read, R. Shah, B. Riley, J. Park, K. Brorson, A. Rathore, Biotechnol. Bioeng., 105 (2010) 285.
[23] E.K. Read, J.T. Park, R.B. Shah, B.S. Riley, K.A. Brorson, A.S. Rathore, Biotechnol. Bioeng., 105 (2010) 276.
[24] M.-N. Pons, S. Le Bonté, O. Potier, J. Biotechnol., 113 (2004) 211.
[25] A.G. Ryder, J. De Vincentis, B.Y. Li, P.W. Ryan, N.M.S. Sirimuthu, K.J. Leister, J. Raman Spectrosc., 41 (2010) 1266.
[26] B. Li, P.W. Ryan, B.H. Ray, K.J. Leister, N.M.S. Sirimuthu, A.G. Ryder, Biotechnol. Bioeng., 107 (2010) 290.
[27] V.A. Lozano, G.A. Ibanez, A.C. Olivieri, Anal Chim Acta, 610 (2008) 186.
[28] V. Lozano, G. Iba ez, A. Olivieri, Anal. Chim. Acta, 651 (2009) 165.
[29] E. Sikorska, I.V. Khmelinskii, W. Prukala, S.L. Williams, M. Patel, D.R. Worrall, J.L. Bourdelande, J. Koput, M. Sikorski, Journal of Physical Chemistry A, 108 (2004) 1501.
[30] P. Bairi, B. Roy, A.K. Nandi, The Journal of Physical Chemistry B, 114 (2010) 11454.
[31] N.S. Moyon, S. Mitra, The Journal of Physical Chemistry A (2011).
[32] A. Grzelak, B. Rychlik, G. Baptosz, Free Radic. Biol. Med., 30 (2001) 1418.
[33] A. Pirie, Biochem. J., 125 (1971) 203.
[34] A. Pirie, Biochem. J., 128 (1972) 1365.
[35] J. Dyer, S. Bringans, W. Bryson, Photochem Photobiol Sci, 5 (2006) 698.
[36] E. Silva, S. Furst, A.M. Edwards, M.I. Becker, A.E. DeIoannes, Photochem. Photobiol., 62 (1995) 1041.
[37] G.S. Harms, S.W. Pauls, J.F. Hedstrom, C.K. Johnson, Journal of Fluorescence, 7 (1997) 283.
[38] R. Bro, Chemom. Intell. Lab. Syst., 38 (1997) 149.
[39] C. Andersen, R. Bro, J. Chemometr., 17 (2003) 200.
[40] C.K. Remucal, K. McNeill, Environ. Sci. Technol., 45 (2011) 5230.
[41] J. Mizdrak, P.G. Hains, D. Kalinowski, R.J.W. Truscott, M.J. Davies, J.F. Jamie, Tetrahedron, 63 (2007) 4990.
[42] R. Bro, J. Chemometr., 10 (1996) 47.
[43] S.P. Gurden, J.A. Westerhuis, R. Bro, A.K. Smilde, Chemometr. Intell. Lab. Syst., 59 (2001) 121.

A rapid fluorescence based method for the quantitative analysis of cell culture media photo-degradation. A. Calvet, B. Li, and A.G. Ryder. *Analytica Chimica Acta*, 807, 111-119 (2014). **DOI**: 10.1016/j.aca.2013.11.028

Table 1: Summary of the PARAFAC model generated from the AFaa dataset.

4-Component: *AFaa dataset*.

Component	% fit	Ex (nm)	Em (nm)	ID
1	51.73	230/275	350	Trp
2	21.32	230/275	305	Tyr
3	2.05	250/285/325	390-405	~ Py
4	1.43	250/360	460	Photo-products

Table 2: Summary of the MCR-ALS model generated from the AFv dataset.

Component	EV*	Ex (nm)	Em (nm)	ID
1	56.00	360	455	HOK
2	14.84	320	390	Py
3	6.82	340 - 375[3] & 455	525	RF
4	11.25	335 - 350[4]	425	NFK
5	1.29	<315	360	Trp
6	9.75	355	490	LmC

* (% fit X)

Table 3: Summary of results for the models giving best prediction of Trp, Tyr, and Rf using selected EEM regions (see supplemental information for Py and FA).

Analyte	X [(a)]	Y[(b)]	LV	R_{ex} [(c)] (nm)	R_{em}[(c)] (nm)	Pre-P[(d)]	REV [(e)] (%)	REP [(e)] (%)	REPT [(e)] (%)
Trp	Trp, Tyr	Trp	4	220 – 310	285 – 495	C1,C	2.4	4.7	1.3
Tyr	Trp, Tyr	Trp, Tyr	3	220 – 290	305 – 495	C1S2,AS	4.6	4.7	2.9
Rf	RF	RF	3	410 – 475	485 – 600	C1,C	0.9	2.3	4.1

(a) The samples included in the calibration step were subsequently spiked with these analytes

(b) The concentration of these analytes were used in the calibration steps

(c) R_{ex} and R_{em} are the excitation and the emission range defining the sub-sample of the original EEM used.

(d) PreP, Pre-processing on **X**, **Y**. Centering (C or C1), Scaling on mode 2 and/or 3 (S2 and/or 3), Autoscaling (AS).

(e) REC, REV, REP are the relative error of calibration, validation and prediction respectively; those errors are calculated from the RMSEC, RMSEV and RMSEP relatively to the mean of the expected values in each case.

[3] The maximum shift across storage time

[4] The maximum shift across storage time